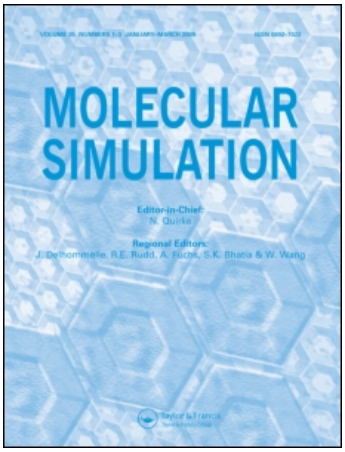

Molecular Simulation
Publication details, including instructions for authors and subscription information:
http://www.informaworld.com/smpp/title~content=t713644482

Structural and vibrational properties of a calcium aluminosilicate glass: classical force-fields vs. first-principles

P. Ganster[a]; M. Benoit[b]; J. -M. Delaye[c]; W. Kob[d]
[a] CRMCN, Marseille Cedex 9, France [b] CEMES, Toulouse Cedex 4, France [c] Laboratoire d'étude du Comportement à Long Terme, CEA Valrhô, Marcoule, Bagnols sur Cèze Cedex, France [d] Laboratoire des Colloïdes, Verres et Nanomatériaux, UMR 5587, Université Montpellier II, Montpellier, France

To cite this Article Ganster, P. , Benoit, M. , Delaye, J. -M. and Kob, W.(2007) 'Structural and vibrational properties of a calcium aluminosilicate glass: classical force-fields vs. first-principles', Molecular Simulation, 33: 13, 1093 — 1103
To link to this Article: DOI: 10.1080/08927020701541006
URL: http://dx.doi.org/10.1080/08927020701541006

Molecular Simulation, Vol. 33, No. 13, November 2007, 1093–1103

Taylor & Francis
Taylor & Francis Group

Structural and vibrational properties of a calcium aluminosilicate glass: classical force-fields vs. first-principles

P. GANSTER†*, M. BENOIT‡, J.-M. DELAYE¶ and W. KOB§

†CRMCN, Campus de Luminy case 913, 13288 Marseille Cedex 9, France
‡CEMES, 29 rue Jeanne Marvig, BP 94347, 31055 Toulouse Cedex 4, France
¶Laboratoire d'étude du Comportement à Long Terme, CEA Valrhô, Marcoule, BP 17171, 30207 Bagnols sur Cèze Cedex, France
§Laboratoire des Colloïdes, Verres et Nanomatériaux, UMR 5587, Université Montpellier II, Place E. Bataillon, 34095 Montpellier, France

(Received March 2007; in final form June 2007)

Using classical and *ab initio* molecular-dynamics (MD) simulations, we have studied a calcium aluminosilicate glass of composition $(SiO_2)_{0.67}-(Al_2O_3)_{0.12}-(CaO)_{0.21}$. Samples with 100 and 200 atoms were generated by classical MD simulations using a potential with 3-body interactions. Although we observe, for the model with 100 atoms, finite size effects for some structural properties, these effects are substantially reduced if the glass structure is refined by the *ab initio* MD simulations. In addition, some structural characteristics such as the Ca—O bond length and the angular distributions are improved by the *ab initio* description. The structural and vibrational characteristics of these glass samples are compared to that of a glass that has been quenched from the melt using first-principles simulations. The main differences are found on the SiOSi and SiOAl angular distributions and on the apparition of high-frequency bands in the partial Ca vibrational density of states for the classically generated glass samples.

Keywords: Glasses; Molecular-dynamics simulations; Car–Parrinello method; Calcium aluminosilicate; Finite size effects

1. Introduction

Aluminosilicate glasses are ubiquitous materials in nature (volcanic magma) as well as in daily life since they form the basis of most of the industrial glasses (windows, bottles, glass for waste confinement, etc.). Nevertheless, the way the macroscopic properties of these systems depends on their microscopic structure is only understood poorly mainly because the experimental determination of the local structure remains a challenging problem due to the lack of positional order.

To date, the calcium aluminosilicate glasses (CAS) are known as being made of silicon and aluminum having a tetrahedral coordination with oxygen atoms [1], the tetrahedra being connected by shared oxygen atoms (named bridging oxygens (BO)) [2]. The tetrahedra form a disordered network in which Ca atoms are randomly distributed. Depending on the Al_2O_3/CaO ratio, the Ca atoms play the role of modifiers if they create non-bridging oxygen (NBO) by breaking TOT links (T = Si/Al) and/or they play the role of charge balancing, by neutralizing the AlO_4^- entities. The viscosity of molten silicates is known to depend strongly on the concentration of the NBO atoms in the system, the latter depending on the Al_2O_3/CaO ratio [3,4]. For a Al_2O_3/CaO ratio equal to one, if we suppose that all the Ca atoms are charge balancing the AlO_4^- entities, no NBO atoms should exist and the viscosity should be maximum. However, an excess number of NBO atoms has been found in some aluminosilicate glasses having a Al_2O_3/CaO ratio equal to one [5], explaining the observed viscosity anomaly in these systems [3,4,6]. This excess number of NBO atoms should be related to the existence of other structural units such as oxygen triclusters and/or highly coordinated Si and Al atoms.

The points discussed above raise some questions concerning the structure of the CAS glasses. In such complex glasses, structural information are not easy to extract from experiments because of the lack of positional order. Computer simulations are therefore very appropriate as an additional tool for the interpretation of experimental data. However in this particular case, computer simulations encounter two kinds of difficulties: (i) In order to properly describe the glassy state, the

*Corresponding author. Email: ganster@crmcn.univ-mrs.fr

Molecular Simulation
ISSN 0892-7022 print/ISSN 1029-0435 online © 2007 Taylor & Francis
http://www.tandf.co.uk/journals
DOI: 10.1080/08927020701541006

systems must be large and good statistics is needed which require the use of empirical potentials and classical molecular-dynamics (MD) simulations that can be carried out on quite large systems and on long times [7]; (ii) For a good description of the chemical bonding (covalent for SiO and AlO and ionic for CaO), accurate electronic structure calculations have to be used, such as the ones based on density functional theory (DFT), which limits the simulations to small systems because of the high computational cost.

This "dilemma" lead us to pursue a series of studies on the CAS systems in which the glasses are generated in different ways. The composition of the studied glasses (21% CaO—12% Al_2O_3—67% SiO_2) was chosen in order to mimic that of the protective layers obtained after the water leaching of the nuclear wastes confinement glasses [8–12]. In Ref. [13], we presented the structural characteristics of a small CAS glass generated with first-principles simulations by quenching from the melt and in Ref. [14], we studied the finite size effects in CAS glasses generated by classical MD using an empirical potential with 2- and 3-body terms. In this later investigation, we observed finite size effects in some of the structural properties of the smallest system made of 100 atoms such as the Si—O, Al—O and Ca—O first neighbor distances, the Si—O—Si and Si—O—Al angular distributions and the nature of the calcium environment.

In this paper, we present the study of the structural properties of CAS glasses that were obtained from classical MD simulations for small systems sizes and that have been subsequently relaxed using *ab initio* simulations of the Car–Parrinello type [15]. This approach has already been successfully used for the study of SiO_2 and $Na_2O–4SiO_2$ glasses and has proved to be useful for the understanding of the limits of the classical potentials [16–20]. The structural properties of the glasses as well as their vibrational properties are also compared to those of a CAS glass generated from quench from the melt first-principles simulations [13].

In the present work, we intend to show that the relaxation of a classically generated glass can substantially improve some of the local structural characteristics but that some other properties, in particular the vibrational ones, will keep the "memory" of the way the glass was generated. This latter fact can become a crucial point, especially in complex system for which the empirical potentials show some limits.

In the next section we give the details of the classical and *ab initio* simulations, then we present the results on the structural properties of the glasses in the third section and the vibrational properties in the fourth section. A discussion of the results and a conclusion are given in the last section.

Table 1. Structural characteristics of the studied samples.

	Sample I	*Sample II*	*Sample III*
Number of atoms	100	100	200
Box edge length (Å)	11.32	11.32	14.26
Si coordination	All SiO_4	All SiO_4	All SiO_4
Al coordination	All AlO_4	All AlO_4	All AlO_4
Ca coordination	~5	~6	~6
Percentage of NBO	9.5	11.1	9.5
Percentage of O triclusters	0.0	1.6	0.0

2. Glass samples preparation

Two liquids of 100 atoms (samples I and II) and one liquid of 200 atoms (sample III) of composition 21% CaO—12% Al_2O_3—67% SiO_2 (in mole %) were equilibrated at 4200 K during 1.8 ns by means of classical MD simulations using a potential made of 2- and 3-body interactions (see Ref. [14] for details about these simulations). The liquids were subsequently quenched to 300 K at a rate of 10^{13} K $s^{-1}$and the obtained glasses were simulated in the NVE ensemble at 300 K during 300 ps. In table 1 we summarize the main structural characteristics of the obtained glass samples, that will be hereafter called "EP" samples (for Empirical Potential). The NBO atoms are defined as oxygen atoms that are connected to only one network-former atom (Si or Al) and the O triclusters are defined as oxygen atoms that are connected to three network-former atoms. By connected we mean that the distance between the two atoms is less than the location of the first minimum after the corresponding radial distribution function (RDF) $g_{\alpha\beta}(r)[\alpha, \beta \in$ Si, O, Al, Ca]. The chosen distance cutoffs used to define the connectivity of the atoms are given in table 2.

The final coordinates and velocities of these classical simulations were then taken as the initial ones for *ab initio* MD simulations of the Car–Parrinello type using the CPMD code [21]. Immediately after the start of the CPMD simulation, we observe a heating of the samples of $\approx$ 200 K as it is shown in figure 1 for one of the 100-atoms system (sample I).

This increase of temperature is the consequence of the modification of the potential when switching from the classical to the *ab initio* description. It is remarkable that the relaxation of the positions when the *ab initio*

Table 2. Distance cutoffs used for determining the nearest neighbours.

	Sample I		*Sample II*		*Sample III*		
	EP	*EP + CP*	*EP*	*EP + CP*	*EP*	*EP + CP*	*"Full" CP*
SiO	2.00	2.00	2.00	2.00	2.00	2.00	2.00
AlO	2.10	2.10	2.24	2.20	2.25	2.14	2.17

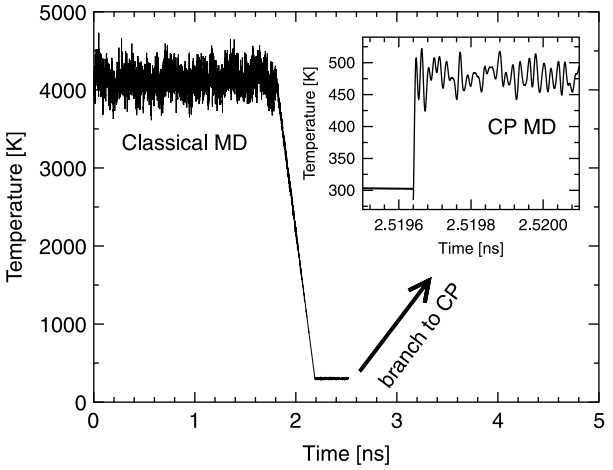

Figure 1. Time evolution of the ionic temperature, defined via the kinetic energy of the atoms, during the classical MD generation of a 100-atoms glass sample (sample I) and the following Car–Parrinello MD simulation (inset).

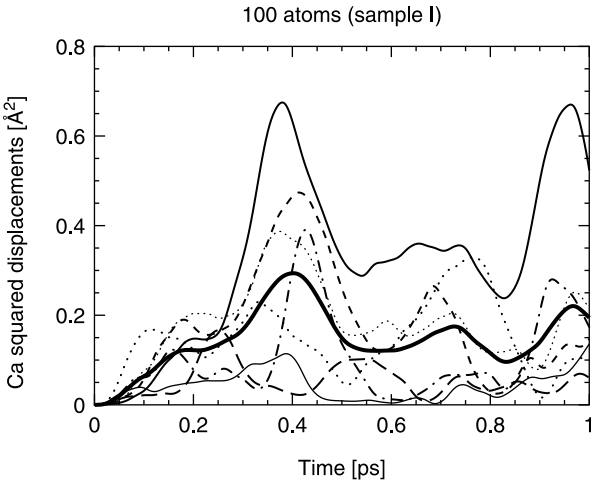

Figure 2. Evolution of the squared displacement of individual Ca atoms during the CP simulation of a 100-atoms system (sample I). Each line corresponds to the squared displacement of a single Ca atom and the thick line corresponds to the mean squared displacement of the Ca atoms.

calculation is started takes only a few MD steps (approximately 80 steps). This procedure was carried out on the two different 100-atoms glasses and on the 200-atoms one. In all three cases, we continued the CP dynamics in the NVE ensemble during $\sim$ 1 ps using the CPMD code. These samples will hereafter be called "EP + CP" samples.

In the Car–Parrinello simulations, the electronic structure was described within the framework of DFT [22] with the generalized gradient approximation employing the B-LYP functional [23,24]. Core electrons were replaced by a Troullier–Martins pseudopotential for oxygen atoms and by Goedecker–Hartwigsen pseudopotentials for the silicon, aluminum and calcium atoms [25]. For the calcium, we have taken into account explicitly semi-core electrons. The electronic wave functions have been expanded at the Γ point of the supercell on a plane waves basis set with an energy cutoff of 80 Ry. The equations of motion were integrated with a timestep of 0.12 fs and a fictitious electronic mass of 600 a.u. was used.

In addition, these samples have also been compared to another CAS glass sample that has been generated from full *ab initio* MD simulations, i.e. for which the liquid equilibration at 3000 K and the linear quench at a rate of 3.6×10^{14} K s have been performed using the CPMD code instead of the classical potential described above. This glass has the same composition and the same number of atoms than the 100-atoms samples I and II and its structural characteristics have been published elsewhere [13]. The only additional difference between this sample (hereafter called "full" CP) and samples I and II is the density, which is slightly lower in the "full" CP case ($2.36\,\mathrm{g\,cm^{-3}}$ instead of $2.42\,\mathrm{g\,cm^{-3}}$).

After switching on the CP simulations, the Si, Al and O atoms did not show significant displacements neither in the 100-atoms nor in the 200-atoms systems. Thus during the CP simulations, the network connectivity is not changed: The Si and Al coordinations, the number of NBO and oxygen triclusters and the number of linkages are conserved. However, we have noted that the Ca atoms underwent larger displacements during the CP simulations as can be seen from figure 2 which shows the squared displacements of each Ca atoms for one of the 100-atoms systems (sample I). From this figure we recognized that the Ca atoms reach equilibrium after 0.3 ps approximately, with a maximum displacement of ≈ 0.6 Å^2 for one of the calcium atoms. After this time, the squared displacements showed oscillations which indicates that the Ca atoms move in their potential energy wells. A similar behaviour was observed in the second 100-atoms sample as well as in the 200-atoms sample.

Once the CP simulation has started, slight structural modifications can be observed in the CAS samples. The major ones are described in the next section and compared to the structural characteristics of the "full CP" sample for the 100-atoms case. We would like to stress the point that the difference in temperature between the EP and EP + CP samples ($\approx$180 K) is not sufficient to explain the differences we find in the structural properties. Indeed previous works [16,17] have already shown that the structural properties of silicates, deep in the glass, are not affected by temperature differences of the order of 100–200 K.

In the 100-atoms case, all the structural characteristics presented in the next subsections have been computed by averaging over the two independent samples.

2.1 Radial distribution functions

The partial RDF [26] have been evaluated during the classical MD and the CP simulations for the different samples of 100 and 200 atoms. The results for the SiO, AlO and CaO RDFs are presented in figure 3 for the EP 100- and 200-atoms samples (figure 3(a)) and for these samples after the CP relaxation (figure 3(b)).

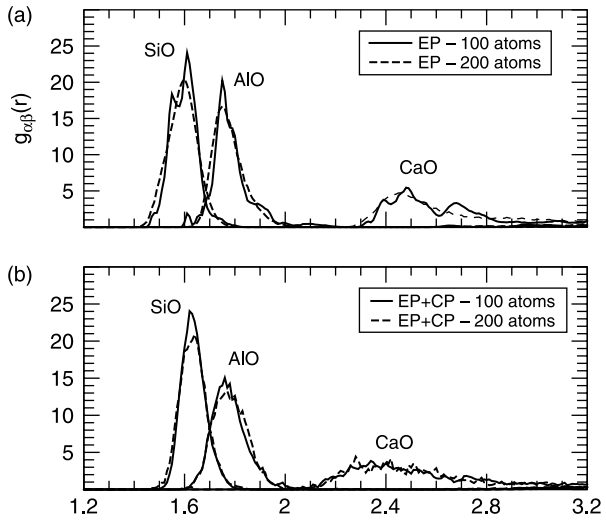

Figure 3. (a) RDF SiO, AlO and CaO for the 100-atoms (bold lines) and 200-atoms (dashed lines) glasses in the classical MD case. (b) RDF SiO, AlO and CaO for the 100-atoms (bold lines) and 200-atoms (dashed lines) glasses after the CP relaxation.

From figure 3(a), one can see that the first peak of the SiO RDF has a different shape in the 100 and the 200 atoms samples. In the 100-atoms case, the peak is splitted in two contrary to the 200-atoms case. As a consequence, it is difficult to assign a most probable SiO interatomic distance in the 100-atoms case whereas it can be defined to 1.60 Å in the 200-atoms case. These size effects have already been analysed in a previous work [14] but the interesting point is that they disappear when the system is relaxed in the *ab initio* description. Indeed, the SiO RDF presented in figure 3(b) no longer presents a double peak in the 100-atoms case. Moreover, for both system sizes, the position of the peak is shifted to 1.63 Å in good agreement with experimental values (1.60–1.63 Å [27–29]). The SiO distance is improved by the CP relaxation.

The origin of the double peak in the SiO RDF for the EP 100 atoms glass can be attributed to oxygens involved in the Si—BO—Al and Si—NBO units. Indeed, from figure 4(a), one can see that the double peak can be decomposed into contributions coming from oxygen atoms involved in Si—NBO and Si—BO—Al for the first peak and from atoms involved in Si—BO—Si for the second peak. The double peak disappears when the Car–Parrinello simulation is switched on, and for the 200-atoms system in the EP and EP + CP cases. In the EP + CP cases, one can see that the difference between the Si—BO—Al and the Si—BO—Si distances is not as important as in the EP case. The existence of the double peak is therefore due to a combined effect of both the small system size and the potential.

The location of the first peak of the AlO RDF (figure 3(a)) is not strongly modified when the CP description is switched on (figure 3(b)), neither in the 100-atoms nor in the 200-atoms cases, but its width is slightly increased. The most probable AlO distance is consequently equal to≈1.77 Å for all system sizes in the EP + CP simulations, which is in good agreement with the experimental value lying between 1.72 and 1.78 Å [27–30].

Finally, in figure 3(a), one can observe no size effects but compared with figure 3(b) a significant change in the CaO RDF arises: The first peak is substantially moved toward smaller distances in the EP + CP simulation for both system sizes and no double peak exists anymore. We thus estimated the most probable CaO distance to be around 2.34 Å for the 100-atoms systems and around 2.36 Å for the 200-atoms system. This distance is much smaller than the one extracted from the classical MD simulations (≈2.50 Å) but in very good agreement with

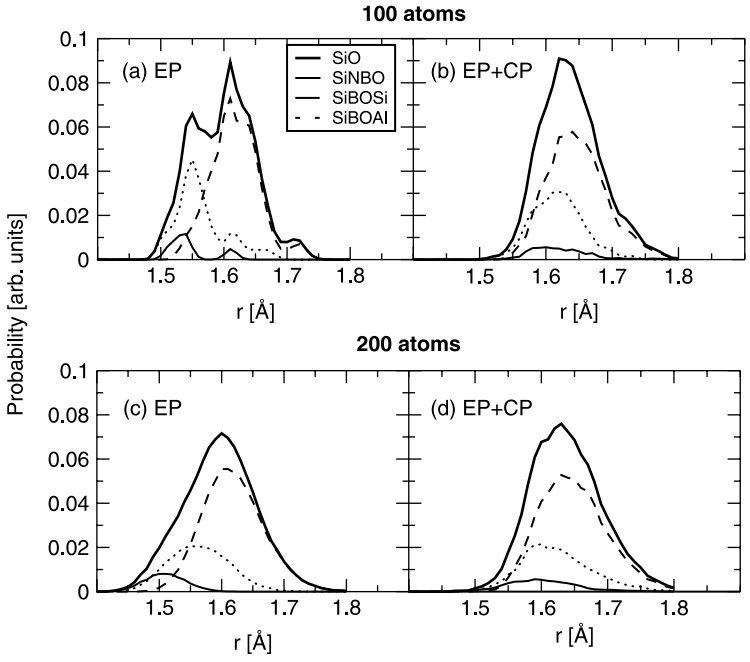

Figure 4. Distributions of the SiO distances decomposed in contributions from oxygen atoms involved in the Si—BO—Si, Si—BO—Al and Si—NBO units: (a) EP 100-atoms system, (b) EP + CP 100-atoms system, (c) EP 200-atoms system and (d) EP + CP 200-atoms system.

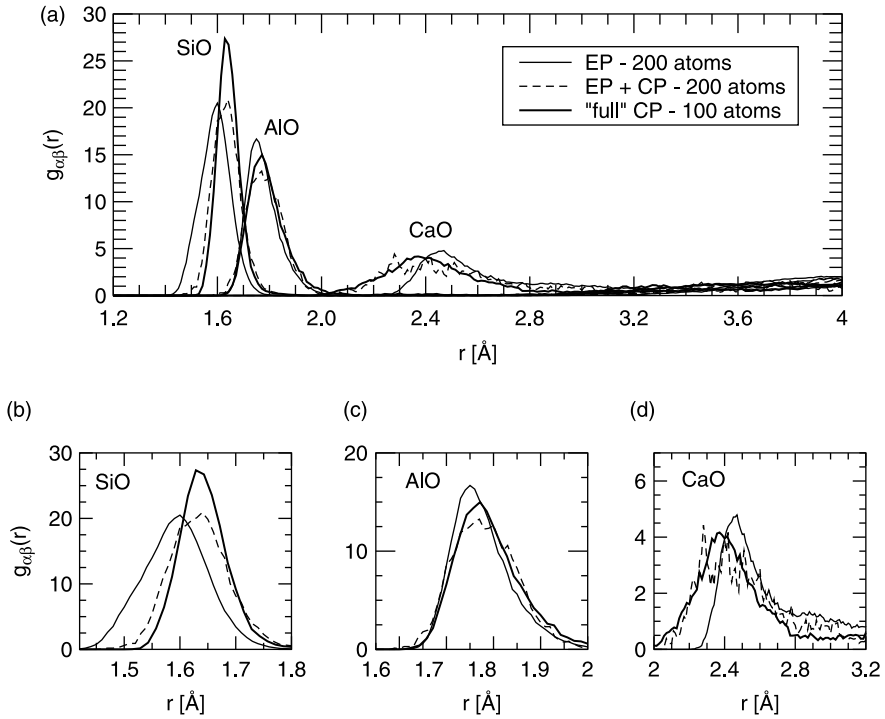

Figure 5. (a) RDF SiO, AlO and CaO of the 200-atoms glasses before (thin lines) and after (dashed lines) the CP relaxation. The bold lines show the same radial distributions functions as obtained from the 100-atoms "full CP" sample. Panels (b)–(d) show magnifications of the RDF first peaks: (b) SiO, (c) AlO and (d) CaO.

experimental estimates which lie between 2.32 and 2.35 Å [28,29].

The RDF after the CP relaxation in the 200-atoms case were compared with the ones obtained from the "full" CP sample, see figure 5. For the SiO and AlO cases, we clearly see that the RDFs after the CP relaxation show very little difference with the ones obtained from the "full" CP sample, except for a remaining slight finite size effect, the "full" CP sample containing 100 atoms. The situation is a bit different for the CaO RDF. In this latter case, the CaO RDF first peak presents several small peaks in the EP + CP 200-atoms glass which are not observed in the "full" CP sample. In general, though, a simple CP relaxation at low temperature seems to be able to correct the first neighbour distances, since these ones are very similar to the ones obtained in the "full" CP sample. This result also shows that one can generate a glass using an empirical potential and refine its structure with *ab initio* calculations, if the only properties of interest are the local structural ones.

In all samples, we tried to evaluate the coordination distributions of the Ca atoms, i.e. the number of oxygen neighbours around the Ca atoms. However given the poor statistics of the CaO RDFs (figure 3(a)), it is very difficult to make a reasonable choice for the cutoff radii and therefore to obtain reliable coordination distributions. Nevertheless we observed a systematic shift of the mean Ca coordination numbers toward smaller values (5 or 6) when the structure is refined by the CP simulations in the 100-atoms systems as well as in the 200-atoms one (not shown). Unfortunately it is rather difficult to obtain from experiments precise values for this coordination number. Values of 4.7 and 5.3 are found from X-ray diffraction [28,29] which are in agreement with the data obtained after the CP relaxation.

2.2. Angular distributions

The angular distributions have been computed for some of the atomic triplets forming a local neighbourhood (SiOSi, SiOAl, AlOAl, OSiO and OAlO). For this we defined two atoms to be neighbours if their distance was less that the location of the minimum in the corresponding partial RDF (values are given in table 2).

Figure 6 shows the evolution of the mean values of the SiOSi, SiOAl, OSiO and OAlO angles as a function of time, during the classical MD simulation and the CP simulation, averaged over the two 100-atoms samples. The mean values of OSiO and OAlO angles for the classical simulation are the same as the ones obtained from the *ab initio* description. A similar behaviour of the mean values of the angles upon switching to the CP simulations was observed in the 200-atoms sample (sample III).

In similar studies of SiO_2 and $NaSi_4O_8$ glasses it has been already observed that the CP description tends to close the SiOSi angles and consequently to shift the SiOSi distribution to smaller angles [16,17]. In figure 6, the phenomenon is observed again since the mean angles for SiOSi and SiOAl decrease by roughly 10° as soon as the CP simulation is started.

The modifications of the mean angular values are accompanied by a global modification of the shape of the angular distributions, as it is demonstrated in figure 7 for

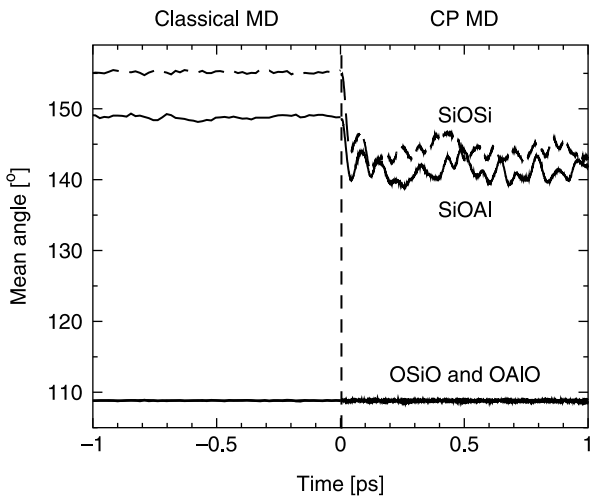

Figure 6. Time evolution of the mean values of the SiOSi, SiOAl, OSiO and OAlO angular distributions during the classical simulation and during the CP simulation, averaged over the two 100-atoms samples.

the 100- and 200-atoms samples. For both sizes, the SiOSi and SiOAl angular distributions (figure 7(b),(c),(g) and (h)) are both shifted to lower angles due to the CP relaxation in agreement with the results of figure 6. In these cases, one can also note that firstly, the distribution is smoothed by the CP simulation and secondly, that it is more probable to find angles smaller than 130° in the *ab initio* than in the classical description. Interestingly, the narrow peaks that are observed in the 100-atoms SiOSi and SiOAl angular distributions, generated by classical MD simulations (figure 7(b),(c)), are completely smeared out when the CP description is switched on (Figure 7(g),(h)). This result corroborates what we found in Ref. [14]: The finite size effects observed in the angular distributions for the 100-atoms systems are due to the use of the 3-body potentials. Therefore, the CP simulation is able to reduce quite substantially the finite size effects created by the use of the 3-body potentials in the 100-atoms system case.

The AlOAl angular distribution (figure 7(a),(f)) is also quite modified by the CP refinement in the 100-atoms case since the narrow peaks are smoother and broader. These small peaks observed in the EP 100-atoms case are due, for the one part, to the very poor statistics (there are only very few AlOAl triplets in the system) and for the second part, to the fact that these angles are quite constrained in the classical case compared to the CP one. Indeed, such a situation is not observed in the 200-atoms system, even in the EP case, since the AlOAl angles present a broad distribution. Finally we would like to point out that the angular distributions obtained for the EP + CP 200-atoms samples are, within the noise of the data, similar than that obtained for the 100-atoms samples. Thus we can conclude that, for this quantity as well, the CP relaxation is able to remove the finite size effects.

In figure 8, we compare the EP and EP + CP 200-atoms angular distributions to that of the 100-atoms "full" CP and we observe that the SiOSi and SiOAl distributions show quite a different shape: They are shifted to lower angles and are narrower with an asymmetric shape. The main peaks are around 130 and 120°, respectively, with a long tail toward larger angles. The fact that the angular distributions are peaked at smaller angles can be firstly attributed to the very high quench rate that was used to generate this sample. Indeed it has been found, from classical MD simulations carried out on silica [31,32], that the use of a high quench rate induces a shift of the SiOSi angular distribution toward smaller angles. However, this shift is of the order of$\approx 5°$ for a quench rate going from 4.44×10^{12} to $1.14 \times 10^{15}\,\mathrm{K\,s^{-1}}$. In the present case, the difference between the quench rates is even smaller (1×10^{13} and $3.6 \times 10^{14}\,\mathrm{K\,s^{-1}}$). Therefore the difference in shape of the SiOSi and SiOAl angular distributions is likely not only due to the difference in quench rates but also to the method of preparation, i.e. to the potential used during the liquid equilibration and the quench. Moreover this result is consistent with the fact that the samples generated classically and relaxed with CP exhibit SiOSi and SiOAl angular distributions which are "in between" the classical ones and the "full" CP ones. This means that the CP relaxation tries to lower the SiOSi angles but, because of the too low temperature (around 480 K), can not fully relax the sample structure and as a result the angular distributions are only shifted by$\approx 10°$. The comparison of the SiOSi and SiOAl angular distributions with experiments is unfortunately not possible since those distributions are not directly accessible. However it is known that the SiOAl angular distribution should be shifted to smaller angles compared to the SiOSi one [33], in agreement with our findings.

In the case of the OSiO and OAlO angular distributions (figure 7(d),(e),(i) and (j)), the peaks are not modified except for a slight spreading in the CP cases compared to the classical ones.

2.3. Structure factors

The neutron structure factors $S_n(q)$ were computed using:

$$S_n(q) = \frac{1}{\sum_\alpha N_\alpha b_\alpha^2} \sum_{\alpha\beta} b_\alpha b_\beta S_{\alpha\beta}(q), \qquad (1)$$

$$\text{with } S_{\alpha\beta}(q) = \frac{f_{\alpha\beta}}{N} \sum_{l=1}^{N_\alpha} \sum_{m=1}^{N_\beta} \langle \exp(i\mathbf{q}\cdot(\mathbf{r}_l - \mathbf{r}_m)) \rangle \qquad (2)$$

Here $\mathbf{q}$ is the scattering vector, N the number of atoms, N_α and N_β the number of atoms of species α and β, respectively. The factor $f_{\alpha\beta}$ is equal to 0.5 for $\alpha \neq \beta$ and equal to 1.0 for $\alpha = \beta$, b_α and b_β are the neutron scattering lengths of species α and β, and are equal to 4.149, 5.803, 3.449, 4.700 fm for Si, O, Al and Ca (www.ncnr.nist.gov/resources/n-lengths/elements/).

In Ref. [14], we compared the neutron structure factors $S_n(q)$ computed for 100- and 1600-atoms CAS glasses and found no differences in the peak positions nor in the peaks intensities between the two system sizes. This result

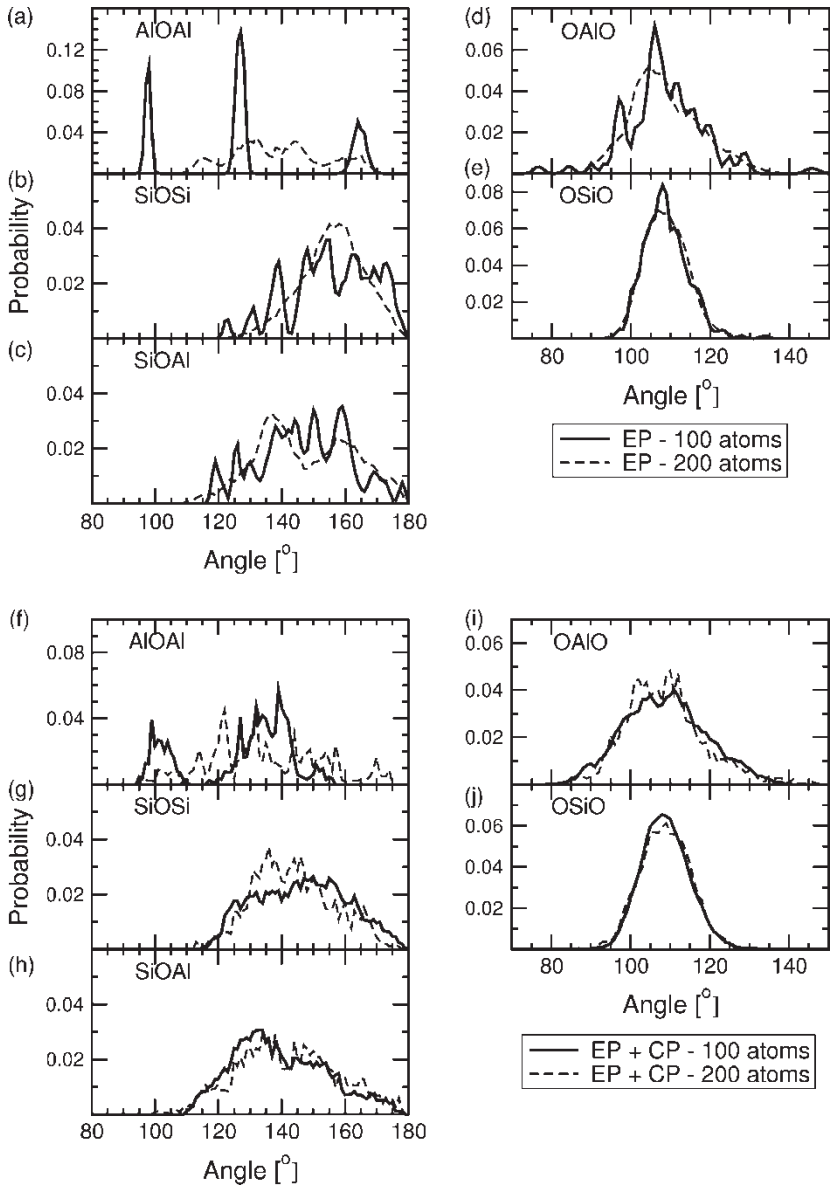

Figure 7. Upper graphs: Distributions of angles for the 100-atoms (bold lines) and 200-atoms (dashed lines) glasses in the classical MD case: (a) AlOAl, (b) SiOSi, (c) SiOAl, (d) OAlO and (e) OSiO. Lower graphs: Distributions of angles for the 100-atoms (bold lines) and 200-atoms (dashed lines) glasses after the CP relaxation: (f) AlOAl, (g) SiOSi, (h) SiOAl, (i) OAlO and (j) OSiO.

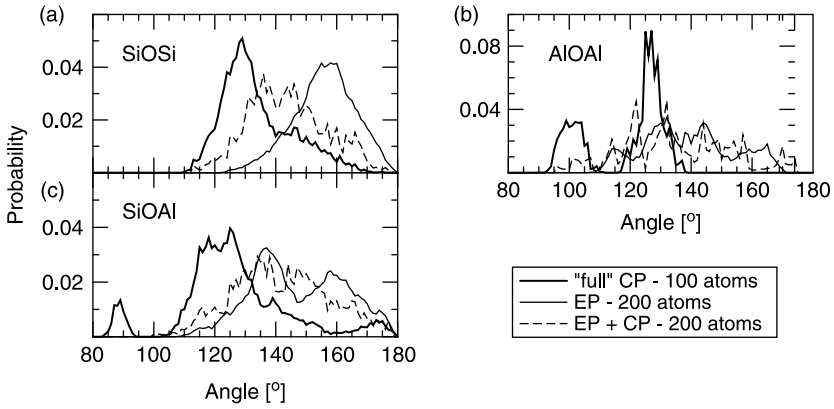

Figure 8. Distributions of angles for the 200-atoms before (thin lines) and after (dashed lines) the CP relaxation and compared to the "full" CP distributions (bold lines): (a) SiOSi, (b) AlOAl and (c) SiOAl.

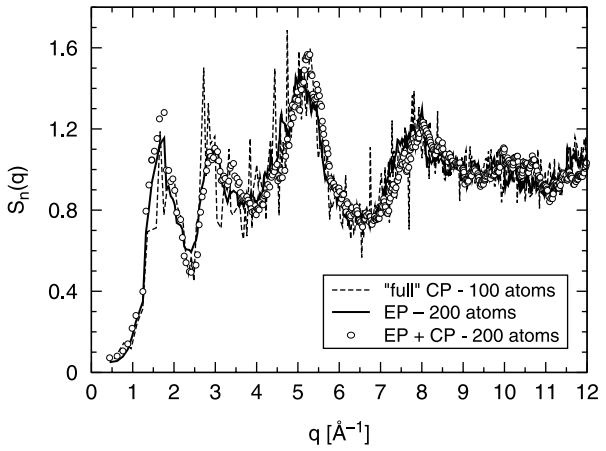

Figure 9. Neutron structure factors of the CAS glass for the 200-atoms systems before (bold lines) and after (circles) the CP relaxation and for the "full CP" samples (thin-dashed lines).

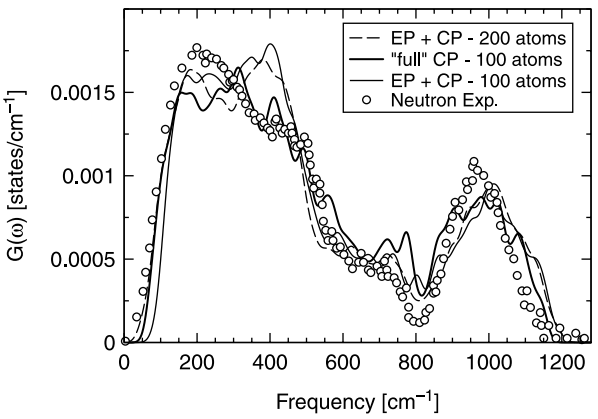

Figure 10. Neutron density of states $G(\omega)$ for the 100-atoms (thin lines) and 200-atoms (dashed lines) glasses after the CP relaxation and for the "full" CP glass sample (bold lines) compared to neutron experiment data from Ref. [34] that were obtained for a glass of composition $(SiO_2)_{0.43}-(CaO)_{0.43}-(Al_2O_3)_{0.14}$.

indicates that the finite size effects do not affect the $S_n(q)$. In the present study, we have computed the $S_n(q)$ for the 200-atoms glasses in the classical MD case and after the CP relaxation and compared the result to the $S_n(q)$ obtained in the "full" CP case (figure 9).

From figure 9, we can see that the most noticeable effect of the CP relaxation on the structure factor is a slight shift of the third peak toward smaller values of q. This effect is slightly enhanced in the case of the 100-atoms systems (not shown here). This third peak is due to the OO and SiO correlations and a shift of this peak toward smaller values of q implies that the correlations extend over larger distances after the CP relaxation. However the other local structural modifications (bond lengths and angular distributions) due to the CP relaxation are not visible in the structure factors.

The main differences between the 200-atoms $S_n(q)$ and the "full" CP one lie in the first peak. This peak seems to be shifted toward smaller values of q in the "full" CP case and shows a contribution at $\approx 1.0\,\text{Å}^{-1}$ which is absent in the classical glass after the CP relaxation. However because of the poor statistics in this q-range (only a few wave-vectors can be used), we can not draw strong conclusion from this result.

3. Vibrational properties

In the classical case, we have computed the vibrational properties of the 100- and 200-atoms samples from an analytical evaluation of the force derivatives.

In the CP case, the dynamical matrices were obtained by evaluating the second derivatives of the total energy with respect to atomic displacements by taking finite differences of the atomic forces. For this, the samples were relaxed to 0 K by a conjugated gradient simulation performed in the *ab initio* description using the CPMD code, at the end of the CP relaxation. The vibrational frequencies and the corresponding eigenmodes were then obtained by diagonalizing the dynamical matrices.

The classical VDOS for the 100- and 200-atoms samples were found to be very different than that obtained after the CP relaxation and are therefore not shown. Indeed they presented a broad band ranging from 50 to 1100 cm^{-1} and a second small band between 1100 cm^{-1} and 1400 cm^{-1}. The differences between the classical VDOS and the *ab initio* ones resemble the ones that have been observed on the amorphous silica VDOS in Ref. [19]. In that paper, not only the VDOS computed using a classical potential and using *ab initio* calculations were different but also the nature of the vibrational eigenmodes. It is very likely that the same kind of discrepancies are found in the present system. The physical nature of these bands will be discussed where the partial VDOS are presented (figure 11).

In figure 10 we show the vibrational densities of states (VDOS) for the 100-atoms (dashed line) and the 200-atoms (thin line) systems after the CP relaxation, and for the "full" CP system (bold line) and compared these results with experimental neutron data (circles) from Ref. [34]. For the 100-atoms systems the data were averaged over the two samples. In order to compare our results to the neutron data, we have computed for each sample the $G(\omega)$, defined as:

$$G(\omega) = C(\omega)g(\omega),$$

where $g(\omega)$ is the VDOS and the coupling constant $C(\omega)$ was computed using the incoherent approximation following Ref. [35]. (Note that the calculations were done at 0 K whereas the experiment was made at 300 K). The functions $C(\omega)$ as obtained for the four samples are found to be very similar and the theoretical $G(\omega)$ reproduce the main experimental features quite well, apart from the high frequency modes above 1200 cm^{-1} which might simply be noise, or be related to impurities in the sample. All three VDOS exhibit a main band between 50 and 500 cm^{-1}, a second band, less intense, around 700 cm^{-1} and a third band at higher frequency, between 800 and 1200 cm^{-1}. The main features of these VDOS can

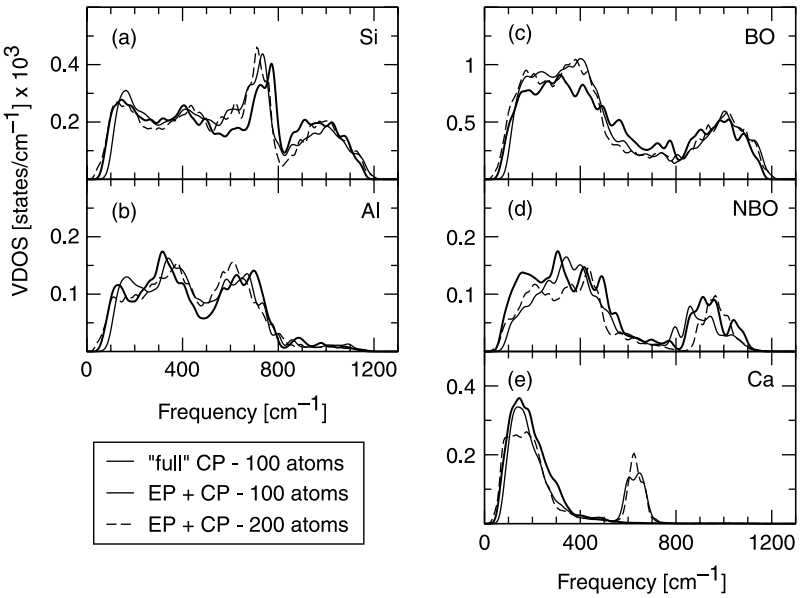

Figure 11. Total and partial vibrational density of states for the 100-atoms (thin lines) and 200-atoms (dashed lines) glasses after the CP relaxation and for the "full" CP glass sample (bold lines).

be found in a large variety of silicate glasses, such as the sodo-silicate ones. In particular, the VDOS obtained from very similar simulations carried out by Ispas *et al.* on a $Na_2O{-}4SiO_2$ glass presented the same features at the same frequencies [20]. Only the gap between the $700\,cm^{-1}$ band and the other ones seem to be less pronounced in the CAS glass than in the sodo-silicate one.

Although the total VDOS for the EP + CP samples are very similar, there are, however, small discrepancies with that obtained with the "full" CP one. Between 150 and $450\,cm^{-1}$ the intensity is lower in the "full" CP case, and the maximum of the high frequency band is slightly shifted toward higher frequencies in the EP + CP case for both system sizes. These differences result in a better agreement of the "full" CP sample $G(\omega)$ with the experimental one, compared to that of the classically generated samples. Thus the vibrational properties keep the memory of the way the glass was generated, as the angular distributions do (see Section 2.2). One could relate this result to the observed effects of the densification on the Raman spectra of amorphous silica [36] for instance, which shows that the vibrational properties of the glass have a memory of the glass history. Our findings are also in agreement with the study of Vollmayr *et al.* who showed by computer simulations that, in amorphous silica, the position of the peak at high frequency shifts to higher frequency when the quench rate is increased [31]. Indeed the cooling rate used for the EP + CP samples is one order of magnitude smaller than that used for the "full" CP sample. However, in the present work, too many parameters are different between the compared samples (cooling rate, interatomic potential, density ...) which prevents to draw any strong conclusion regarding the reason of the discrepancies between the three $G(\omega)$.

It is instructive to compare the partial VDOS which are defined by:

$$g_\alpha(\omega) = g(\omega)\sum_{i\in\alpha}|\mathbf{e}_i(\omega)|^2$$

where the $\{\mathbf{e}_i\}$ are the 3-components eigenvectors for each atom i of type α. These partial VDOS were computed for the different atom types in all three samples (figure 11): Si, Al, BO, NBO and Ca. The BO atoms are defined as oxygen atoms connected to two network-former atoms (Si or Al) and the NBO atoms are defined as oxygen atoms connected to only one network-former. The same distance cutoffs as in Section 2.2 are used to define the BO and NBO atoms (see table 2). From figure 11, one can see that the main frequency band between 50 and $600\,cm^{-1}$ is mainly due to Si, Al, and BO atoms and are related to breathing modes of rings of connected tetrahedra. At low frequency, the contribution of the Ca atoms is also important (between 50 and $400\,cm^{-1}$ and also at $600\,cm^{-1}$) and resembles the one found for Na in sodo-silicate in Ref. [20]. Finally the high frequency peak is due to bending and stretching modes involving mainly Si, BO and NBO atoms.

From figure 11 we can also conclude that the difference in intensity between 150 and $450\,cm^{-1}$ can be attributed to an intensity difference in the BO (figure 11(c)) and NBO (figure 11(d)) partial VDOS. On the other hand, the shift of the high frequency band seems to be due to the difference between the three BO VDOS at high frequency. Also the Si VDOS seems to contribute in that frequency range. The NBO VDOS are also quite different at high frequency however the intensity is much smaller than that

of the BO and Si VDOS, therefore their contribution to the total VDOS is not the dominant one.

Finally, the most striking difference between the different samples is detected in the Ca VDOS (figure 11(e)). For this species, a main low frequency band is observed around $150\,cm^{-1}$ for all samples, which has a similar origin as the low frequency band observed in the Na partial VDOS of the $Na_2O-4SiO_2$ glass [20]. This band has a tail toward high frequencies which, for the "full" CP sample, vanishes at $\approx 400\,cm^{-1}$. In contrast to this, all the EP + CP samples (100- and 200-atoms) show an additional peak around $\approx 600-700\,cm^{-1}$. These relatively high frequency peak for the Ca atoms is quite intriguing since no similar features were found in the $Na_2O-4SiO_2$ glass [20].

A more detailed analysis of the eigenmodes corresponding to these double peaks showed that the largest part of the mode is localized only on one Ca atom in sample I, on two Ca atoms in sample II and on three Ca atoms in sample III (200 atoms). The fact that this peak is absent in the "full" CP sample lead us to analyse the environment of the Ca atoms in all samples. This study showed, however, that there is no particular characteristics that can be clearly attributed to the Ca atoms responsible for these peaks, neither in their oxygen or calcium environments, nor in the CaO bond lengths. The fact that the samples differ by their mass densities is unlikely to be responsible for the difference in the VDOS for Ca, but this mass difference is only of 2.5%.

In order to explain the existence of this double peak, one therefore should (i) check whether it is systematically present in the CAS glasses generated by classical MD simulations, (ii) check if it is dependent on the quench rate and (iii) find a way to relate its existence to the used empirical potential. However in order to do this, one would have to do extensive new simulations of a large number of samples, with different quench rates, refine them using the CP code and then, compute their vibrational properties from finite differences calculations. This is unfortunately far beyond the scope of the present work because of the large computer resources that would be required. Nevertheless, the fact that this peak is also present in the 200-atoms glass seems to confirm its existence and its relation to the way the glass was generated. And finally, the comparison with the VDOS computed in the $Na_2O-4SiO_2$ glass [20] seems to indicate that this peak is an artifact of the classical MD simulations that the CP refinement is not able to remove.

4. Conclusions

We have studied CAS by MD simulations using an empirical potential and *ab initio* calculations of the forces. Systems of 100 and 200 atoms have been generated using an empirical potential made of 2- and 3-body terms and their structures were subsequently refined by *ab initio* MD simulations of the Car–Parrinello type. We find that the *ab initio* refinement not only improves some of the local structural characteristics (CaO bond length), but also removes the finite size effects observed on the 100-atoms glasses. Therefore the present work gives evidence that the local structure of relatively complex glasses can be studied by the means of *ab initio* simulations using relatively small samples. Preparing a glass by combining classical and *ab initio* MD allows to obtain a glassy network coherent with the one obtained by a full Car–Parrinello calculation. This result is very interesting because the first method is much less time consuming than the second one.

Furthermore we have compared the structures of the classically generated glass samples with a glass sample generated by *ab initio* MD simulations (i.e. the liquid equilibration and the quench were performed using first-principles). Although the bond distances are independent on the way the glasses were generated, the Si—O—Si and Si—O—Al angular distributions are shifted toward smaller angles in the *ab initio* generated glass sample. These angular shifts could be due to a quench effect because the quench rate is faster by a factor of 36 for the sample prepared by a "full" CP calculation.

Nevertheless, the vibrational properties of a glass prepared by a "full" CP calculation remain better, compared to the experimental one, than that of the sample prepared by classical MD and refined by *ab initio*. In particular, in these last samples, a peak is found at $\approx 600\,cm^{-1}$ in the Ca partial VDOS which is absent in the *ab initio* generated glass. The origin of this peak remains unclear.

In conclusion, the present study shows that (i) a glassy structure coherent with a "full" CP calculation can be obtained much more rapidly by combining classical and *ab initio* MD simulations, (ii) some effects of the empirical potentials are not cured by the *ab initio* refinement at low temperature, especially for the Ca vibrational modes. The combination of classical MD and *ab initio* refinement is therefore a promising way to prepare good glass samples, with both good structures and good vibrational properties. Obviously, the better the empirical potentials, the better the final glassy samples will be.

Acknowledgements

Calculations have been performed on the IBM/SP4 at CINES (Montpellier) and on the HP AlphaServer SC 45 at CCRT (Bruyères le Châtel, CEA). Part of this work was supported by the European Community's Human Potential Program under contract HPRN-CT-2002-00307, DYGLAGEMEM.

References

[1] Z. Wu *et al.* Evidence for Al/Si tetrahedral network in aluminosilicate glasses from Al K-edge x-ray-absorption spectroscopy. *Phys. Rev. B*, **60**, 9216 (1999).
[2] B.O. Mysen. *Structure and Properties of Silicate Melts*, Elsevier, Amsterdam (1988).

[3] M.J. Toplis, D.B. Dingwell, T. Lenci. Peraluminous viscosity maxima in Na_2O-Al_2O_3-SiO_2 liquids: The role of triclusters in tectosilicate melts. *Geochim. Cosmochim. Acta*, **61**, 2605 (1997).

[4] M.J. Toplis, D.B. Dingwell. Shear viscosities of CaO-Al_2O_3-SiO_2 and MgO-Al_2O_3-SiO_2 liquids: implications for the structural role of aluminum and the degree of polymerisation of synthetic and natural aluminosilicate melts. *Geochim. et Cosmochim. Acta*, **68**, 5169 (2004).

[5] J.F. Stebbins, Z. Xu. NMR evidence for excess non-bridging oxygen in an aluminosilicate glass. *Nature*, **390**, 60 (1997).

[6] M.J. Toplis, D.B. Dingwell. Viscosity Maxima of Melts Close to the "Charge Balance" Join in the Systems (Na_2O, CaO, MgO) -Al_2O_3-SiO_2: Implications for the Structural Role of Aluminium. *Eos Trans. Am. Geophys. Un.*, **77**, F848 (1996).

[7] R.M. Van Ginhoven, H. Jonsson, L.R. Corrales. Silica glass structure generation for ab initio calculations using small samples of amorphous silica. *Phys. Rev. B*, **71**, 024208 (2005).

[8] S.-B. Xing, A.C. Buechele, I.L. Pegg. Effect of surface layers on the dissolution of nuclear waste glasses. *Mat. Res. Soc. Symp. Proc.*, **333**, 541 (1994).

[9] J.C. Dran, J.C. Petit, C. Brousse. Mechanism of aqueous dissolution of silicate glasses yielded by fission tracks. *Nature*, **319**, 485 (1986).

[10] S. Gin. Protective effect of the alteration gel : A key mechanism in the long term behavior of nuclear waste glass. *Mat. Res. Soc. Symp. Proc.*, **663**, 207 (2000).

[11] F. Angeli, T. Charpentier, S. Gin, J.C. Petit. [17]O 3Q-MAS NMR characterization of a sodium aluminoborosilicate glass and its alteration gel. *Chem. Phys. Lett.*, **341**, 23 (2001).

[12] J.A. Tossel, G. Saghi-Szabo. Aluminosilicate and borosilicate single 4-rings: Effects of counterions and water on structure, stability, and spectra. *Geochem. Cosmochem. Acta*, **61**, 1171 (1997).

[13] M. Benoit, M. Profeta, F. Mauri, C.J. Pickard, M.E. Tuckerman. First-principles calculation of the 0-17 NMR parameters of a calcium aluminosicilate glass. *J. Phys. Chem. B*, **109**, 6052 (2005).

[14] P. Ganster, M. Benoit, J.-M. Delaye, W. Kob. Structural properties of a calcium aluminosilicate glass from molecular-dynamics simulations: A finite size effects study. *J. Chem. Phys.*, **120**, 10172 (2004).

[15] R. Car, M. Parrinello. Unified Approach for Molecular Dynamics and Density-Functional Theory. *Phys. Rev. Lett.*, **55**, 2471 (1985).

[16] M. Benoit, S. Ispas, P. Jund, R. Jullien. Model of silica glass from combined classical and ab initio molecular-dynamics simulations. *Euro. Phys. J. B*, **13**, 631 (2000).

[17] S. Ispas, M. Benoit, P. Jund, R. Jullien. Structural and electronic properties of the sodium tetrasilicate glass $Na_2Si_4O_9$ from classical and ab initio molecular dynamics simulations. *Phys. Rev. B*, **64**, 214206 (2001).

[18] S. Ispas, M. Benoit, P. Jund, R. Jullien. Structural properties of glassy and liquid sodium tetrasilicate: comparison between ab initio and classical molecular dynamics simulations. *J. Non. Cryst. Sol.*, **307–310**, 946 (2002).

[19] M. Benoit, W. Kob. The vibrational dynamics of vitreous silica: Classical force fields vs.first-principles. *Europhys. Lett.*, **60**, 269 (2002).

[20] S. Ispas, N. Zotov, S. de Wispelaere, W. Kob. Vibrational properties of a sodium tetrasilicate glass: Ab initio versus classical force fields. *J. Non. Cryst. Sol.*, **351**, 1144 (2005).

[21] CPMD Version 3.3, J. Hutter, A. Alavi, T. Deutsch, M. Bernasconi, St. Goedecker, D. Marx, M. Tuckerman, M. Parrinello. MPI für Festkörperforschung and IBM Research, (1995–99).

[22] P. Hohenberg, W. Kohn. Inhomogeneous Electron Gas. *Phys. Rev.*, **136**, B864 (1964); W. Kohn and L. Sham, Self-consistent Equations Including Exchange and Correlation Effects. *Phys. Rev.* **140,** A1133 (1965).

[23] A.D. Becke. Density-functional exchange-energy approximation with correct asymptotic behavior. *Phys. Rev. A*, **38**, 3098 (1988).

[24] C. Lee, W. Yang, R.G. Parr. Development of the Colle-Salvetti correlation-energy formula into a functional of the electron density. *Phys. Rev. B*, **37**, 785 (1988).

[25] S. Goedecker, M. Teter, J. Hutter. Separable dual-space Gaussian pseudopotentials. *Phys. Rev. B*, **54**, 1703 (1996); C. Hartwigsen, S. Goedecker and J. Hutter, Relativistic separable dual-space Gaussian pseudopotentials from H to Rn. *Phys. Rev. B*, **58**, 3641 (1998)..

[26] M.P. Allen, D.J. Tildesley. *Computer Simulation of Liquids*, Oxford University Press, Oxford (1989).

[27] G.E. Brown, G.V. Gibbs, P.H. Ribbe. The nature and variation in length of the Si-O and Al-O bonds in framework silicates. *Am. Mineral.*, **54**, 1044 (1969).

[28] V. Petkov, S.J.L. Billinge, S.D. Shastri, B. Himmel. Polyhedral Units and Network Connectivity in Calcium Aluminosilicate Glasses from High-Energy X-Ray Diffraction. *Phys. Rev. Lett.*, **85**, 3436 (2000).

[29] L. Cormier, D. Ghaleb, D.R. Neuville, J.-M. Delaye, G. Calas. Chemical dependence of network topology of calcium aluminosilicate glasses: a computer simulation study. *J. Non.-Cryst. Solids*, **332**, 255 (2003).

[30] N. Jiang, J. Qiu, J.C.H. Spence. Long-range structural fluctuations in a CaO-Al_2O_3-$2SiO_2$ glass observed by spatially resolved near-edge spectroscopy. *Phys. Rev. B*, **66**, 054203 (2002).

[31] K. Vollmayr, W. Kob, K. Binder. Cooling-rate effects in amorphous silica: A computer-simulation study. *Phys. Rev. B*, **54**, 15808 and references therein (1996).

[32] S. Ito, T. Taniguchi. Effect of cooling rate on structure and mechanical behavior of glass by MD simulation. *J. Non.-Cryst. Solids*, **349**, 173 (2004).

[33] G.E. Brown, F. Farges, G. Calas. Structure, dynamics and properties of silicate melts. In *Reviews in Mineralogy*, J.F. Stebbins, P.F. McMillan, D.B. Dingwell (Eds.), **32,** (1995).

[34] J. Zhao, P.H. Gaskell, L. Cormier, S.M. Bennington.Vibrational density of states and structural origin of the heat capacity anamalies in $Ca_3Al_2Si_3o_{12}$ glasses. *Phys. B*, **241–243**, 906 (1998).

[35] S.N. Taraskin, S.R. Elliott. Connection between the true vibrational density of states and that derived from inelastic neutron scattering. *Phys. Rev. B*, **55**, 117 (1997).

[36] P. McMillan, B. Piriou, R. Couty, "A Raman Study of pressure-densified vitreous silica". *J. Chem. Phys.*, **81**, 4234 (1984).